



Detecting Climate Change due to Increasing Carbon Dioxide

Author(s): Roland A. Madden and V. Ramanathan

Source: *Science*, New Series, Vol. 209, No. 4458 (Aug. 15, 1980), pp. 763-768

Published by: American Association for the Advancement of Science

Stable URL: <http://www.jstor.org/stable/1684625>

Accessed: 24/03/2010 23:12

Your use of the JSTOR archive indicates your acceptance of JSTOR's Terms and Conditions of Use, available at <http://www.jstor.org/page/info/about/policies/terms.jsp>. JSTOR's Terms and Conditions of Use provides, in part, that unless you have obtained prior permission, you may not download an entire issue of a journal or multiple copies of articles, and you may use content in the JSTOR archive only for your personal, non-commercial use.

Please contact the publisher regarding any further use of this work. Publisher contact information may be obtained at <http://www.jstor.org/action/showPublisher?publisherCode=aaas>.

Each copy of any part of a JSTOR transmission must contain the same copyright notice that appears on the screen or printed page of such transmission.

JSTOR is a not-for-profit service that helps scholars, researchers, and students discover, use, and build upon a wide range of content in a trusted digital archive. We use information technology and tools to increase productivity and facilitate new forms of scholarship. For more information about JSTOR, please contact support@jstor.org.



American Association for the Advancement of Science is collaborating with JSTOR to digitize, preserve and extend access to *Science*.

<http://www.jstor.org>

Detecting Climate Change due to Increasing Carbon Dioxide

Roland A. Madden and V. Ramanathan

The possible climatic effects of large increases in atmospheric CO₂ due to burning of fossil fuels may constitute one of the important environmental problems of the coming decades. Research efforts are being made to reduce the large uncer-

We first discuss a long time series of surface temperatures and the rationale on which our estimates of the inherent variability or noise are based. Next we present the model results for surface warming due to the CO₂ increase. By

Summary. The observed interannual variability of temperature at 60°N has been investigated. The results indicate that the surface warming due to increased carbon dioxide which is predicted by three-dimensional climate models should be detectable now. It is not, possibly because the predicted warming is being delayed more than a decade by ocean thermal inertia, or because there is a compensating cooling due to other factors. Further consideration of the uncertainties in model predictions and of the likely delays introduced by ocean thermal inertia extends the range of time for the detection of warming, if it occurs, to the year 2000. The effects of increasing carbon dioxide should be looked for in several variables simultaneously in order to minimize the ambiguities that could result from unrecognized compensating cooling.

tainties in estimates of future levels of CO₂ in the atmosphere and in corresponding model predictions of the climatic effects of these new levels. Another important aspect of the problem is our ability to detect climatic effects of increased CO₂, if and when they occur. The inherent variability of climate will make detection of changes due to increasing CO₂ difficult (1). If we consider climate changes due to CO₂ as a "signal," then the inherent variability acts as a "noise." It is our intention in this article to provide some quantitative estimates of this noise and to examine the feasibility of detecting a CO₂ signal.

The authors are staff scientists at the National Center for Atmospheric Research, Boulder, Colorado 80307.

comparing the estimated noise to the largest and the smallest signals predicted by models, we obtain a range of time within which we might expect to detect the effect of increasing CO₂ with some degree of statistical reliability. Uncertainties remain because our current knowledge of climate does not allow us to distinguish between changes due to CO₂ and those not due to CO₂ (2). However, the analysis places the problem in perspective. In order to prove or disprove the existence of the theoretically predicted effects of increasing levels of CO₂, it may be necessary to monitor several variables and formulate arguments based on physical as well as statistical grounds to minimize the effect of the many uncertainties involved.

Data Analysis

Data description. We estimated the noise on the basis of nearly continuous records of observed monthly mean temperatures from 1906 through 1977 for the 12 stations indicated in Fig. 1. Less than 1 percent of the possible 10,368 (12 × 12 × 72) monthly mean temperatures is missing. Values from the 12 stations were averaged to produce zonal mean temperatures that we assume to be representative of 60°N. This latitudinal zone was chosen because long time series of zonal means are more difficult to determine at other latitudes. The number of available stations with long records is more limited farther north and the geographic distribution of stations is less favorable farther south because of the larger percentage of oceans there.

Estimates of the noise. For the time being, we assume that the observed variance in the 72-year record results from factors other than possible effects of increasing CO₂ and, for the purpose of this analysis, is therefore noise (3). Later we will consider the contribution that a CO₂ signal, if it exists, might have made to the total variance over the 72 years. The noise can be reduced by time averaging. Jones (4) pointed out that the variance of time averages depends mainly on the spectral density near zero frequency and not on the total variance of the time series. For that reason, we first estimated the spectrum of the zonal mean temperature values, or their variance as a function of frequency. The data were broken up into five time series: one for each 3-month season (spring corresponds to March, April, and May, and so on) and one 12-month annual mean time series. Autocovariance functions were computed for each series out to a maximum of *M* lags. The autocovariances were then filtered with a Parzen filter (5) and the spectra estimated from the Fourier transform of the filtered autocovariances. The selection of *M*, the maximum lag, involves a compromise between minimizing the variance and minimizing the bias in our spectral estimates. By choosing a small *M* one obtains a small variance or range of statistical confidence limits about the estimated spectra, but

the bias is correspondingly large. Since it is likely that the true spectra fall off with increasing frequency (6), a choice of small M to minimize the confidence limits about the spectral estimates could seriously bias our near-zero spectral estimates downward. We chose $M = 27$, which results in approximately 9.5 degrees of freedom and a standardized bandwidth of 0.069 cycle per year (5). We discuss a likely consequence of bias for this choice of M in a later section.

The resulting spectra are presented in Fig. 2. It is important to note that the variance of 3-month summer means is less than that of 12-month annual means. This is because the variance of winter seasons is so much larger than that of summer seasons. Our basis for estimating the effect of longer time averages on the variance is the relationship between the input and output spectral density functions of a linear system (7); that is,

$$s(f)_N = S(f)|H(f)_N|^2$$

where $s(f)_N$ is, in this case, the power spectral density function of an N -year average of spring, summer, autumn, winter, or annual mean temperatures at frequency f , $H(f)_N$ is the amplitude response of an N -year average, and $S(f)$ is the power spectral density function of

the corresponding seasonal or annual mean temperature.

The variance of an N -year average is given by

$$\sigma_N^2 = \int_{-\infty}^{\infty} s(f)_N df$$

or

$$\sigma_N^2 = \int_{-\infty}^{\infty} S(f)|H(f)_N|^2 df \quad (1)$$

Figure 3 shows $|H(f)_N|^2$ for $N = 2, 10,$ and 30 . The importance of the low-frequency estimates of $S(f)$ in determining σ_N^2 is evident from Eq. 1 and Fig. 3.

From Eq. 1 we estimated σ_N^2 for the four seasonal and annual means for various times N . The results are indicated in Fig. 4, where $2\sigma_N$ is plotted against N . The curves for the four seasons resemble ones with an $N^{-1/2}$ dependence but they do not fall off quite as fast. This is because the seasonal spectra are approximately constant with frequency; that is, they are similar to spectra of uncorrelated data. The spectrum of annual means differs the most from this behavior, having relatively more variance at low frequencies than at high ones. The resulting decrease in variance with increasing averaging time is correspondingly less rapid than that for the seasonal means.

Predicted Climatic Effects and

Estimates of Uncertainty

Radiative heating. Increasing CO_2 , while holding fixed all the other climate parameters that influence the radiation budget, will cause radiative heating of the surface-troposphere system. The hemispheric mean of this radiative heating $\langle \Delta q \rangle$ (angle brackets designate hemispheric mean) due to increased CO_2 can be approximately expressed as (8)

$$\langle \Delta q (\text{W m}^{-2}) \rangle = (5.9 \pm 1) \ln g; \quad (2)$$

$$1 \leq g \leq 2$$

$$g = \text{CO}_2 / \text{CO}_2^0; \quad (3)$$

$$250 \leq \text{CO}_2^0 \leq 330 \text{ ppm}$$

where g is the fractional increase of CO_2 over the reference atmospheric concentration, CO_2^0 . The uncertainty of ± 1 watt per square meter for the constant 5.9 in Eq. 2 is due to possible errors in radiation model calculations (9).

The surface temperature signal. Climate models predict that CO_2 radiative heating warms the surface and troposphere. The increase in hemispheric mean surface temperature $\langle T_s \rangle$ can be expressed as

$$\langle \Delta T_s (\text{K}) \rangle = \frac{\langle \Delta q (\text{W m}^{-2}) \rangle}{\lambda_0 (\text{W m}^{-2} \text{K}^{-1})} \quad (4)$$

where the parameter λ_0 is determined by the feedback processes in the climate system, and has been the subject of considerable research in the last decade. We estimate a reasonable range for λ_0 to be

$$1 \leq \lambda_0 \leq 4 \text{ W m}^{-2} \text{K}^{-1} \quad (5)$$

Most current climate model studies yield λ_0 values ranging from approximately 1 to 2 $\text{W m}^{-2} \text{K}^{-1}$. We consider 4 $\text{W m}^{-2} \text{K}^{-1}$ to be an upper limit because (i) in current climate models mainly positive feedbacks are identified, and (ii) we obtain $\lambda_0 = 4 \text{ W m}^{-2} \text{K}^{-1}$ if we assume that the positive feedbacks are exactly canceled by as yet unidentified negative feedbacks or that the climate system is actually devoid of positive feedbacks (10). Hence in this analysis we will obtain the lower limit for the signal from Eq. 4 with $\lambda_0 = 4 \text{ W m}^{-2} \text{K}^{-1}$ and substituting the lower limit of Δq from Eq. 2. Hereafter, this lower limit will be referred to as the zero-feedback case.

Our interest is in high latitudes, for which we have estimated the noise and where, it turns out, the predicted ΔT_s is much larger than $\langle \Delta T_s \rangle$ (8, 11). The high-latitude amplification is triggered by the coupling between T_s and ice or snow cover—that is, the so-called ice/snow-albedo feedback (11). This amplification is significantly enhanced by the interac-

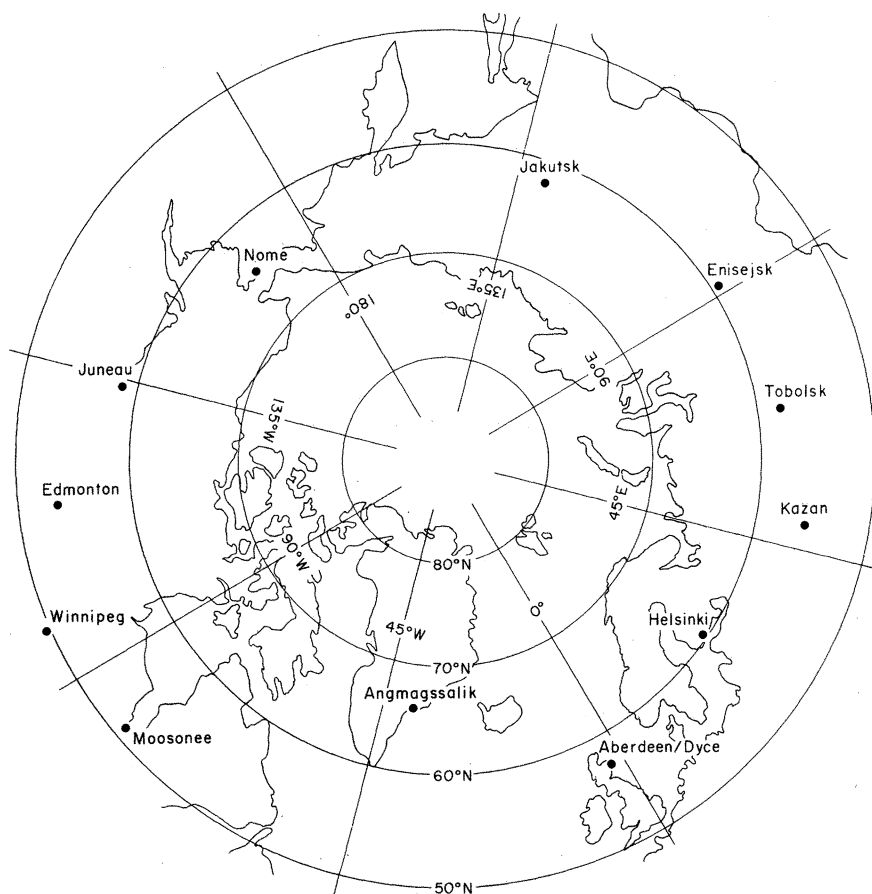


Fig. 1. Stations from which 72-year surface temperature records were taken to compute the approximate 60°N zonal mean.

tions between T_s , atmospheric humidity, lapse rate, and radiative cooling to space (11, 12). For this analysis, we adopt Manabe and Wetherald's (11) general circulation model (GCM) results for high-latitude ΔT_s . For a doubling of CO_2 , their results can be approximately parameterized as

$$\Delta T_s(\theta) \approx 14(1 - 1.4 \cos \theta); \quad \theta > 55^\circ \quad (6)$$

where θ is latitude. Because of the logarithmic dependence of $\langle \Delta q \rangle$ on g (Eq. 2), we can express Eq. 6 as

$$\Delta T_s(\theta) = 20 \ln g(1 - 1.4 \cos \theta); \quad \theta > 55^\circ \quad (7)$$

We adopt Eq. 7 as an upper limit for the signal and refer to it as the positive-feedback case and the upper limit for the positive-feedback case. Manabe and Wetherald's (11) study is for annual mean conditions and hence ignores the seasonal dependence of ΔT_s , which is shown to be significant

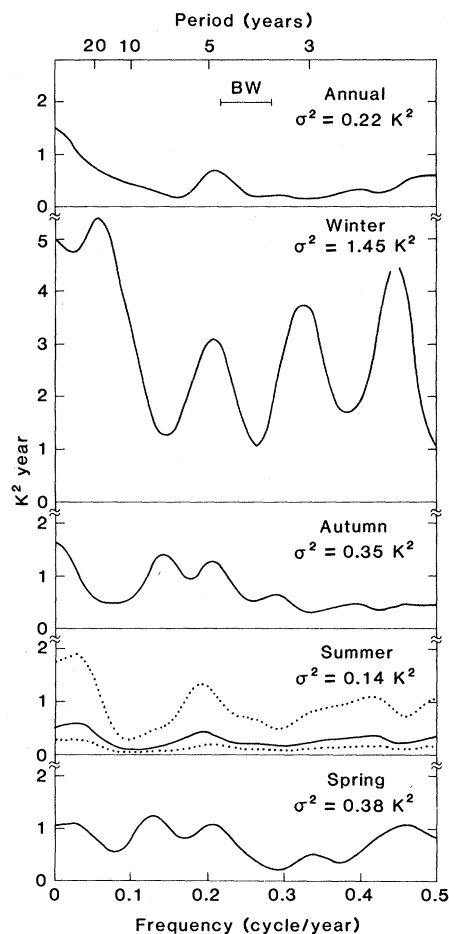


Fig. 2. Spectra $S(f)$ of the seasonal and annual zonal mean temperatures for 60°N . Areas under the spectra are proportional to variance in a given frequency range. The total variance σ^2 is indicated at the upper right, the bandwidth (BW) in the center. Spring, summer, autumn, and annual spectra are based on 72-year records, winter spectra on a 71-year record. Spectra have approximately 9.5 degrees of freedom. The 95 percent limits are indicated by dotted lines for the summer spectra.

by Ramanathan *et al.* (8). Using a seasonal energy balance climate model, Ramanathan *et al.* (8) indicated that the polar amplification occurs mainly during late spring and early summer and the spring-summer maximum in the computed ΔT_s agrees closely with Eq. 7. However, because of the simplified nature of their model, these results should be considered tentative and the expected seasonal variation uncertain.

Our estimate for the range of $\Delta T_s(\theta)$ is given by

$$1.2 \ln g \leq \Delta T_s(\theta) \leq 20 \ln g(1 - 1.4 \cos \theta); \quad \theta > 55^\circ \quad (8)$$

The lower limit is for the zero-feedback case. In using Eq. 4 to obtain the lower limit, we have tacitly assumed that ΔT_s is independent of season and latitude for the zero-feedback case.

Equation 8, relating g to ΔT_s , applies to the equilibrium (or steady-state) response of T_s to g . Since g is a function of time, ΔT_s as given by Eq. 8 should lag in time behind g because of the inertia of the climate system, which is primarily controlled by the thermal inertia of the oceans. This important question has received little attention in the literature, and recent studies employing simplified models of the ocean mixed layer indicate that ocean thermal inertia could delay the surface warming by periods ranging from a few years to a few decades (13).

Scenario for CO_2 increase. To estimate the range of the CO_2 signal we first need an estimate for the time history of g . With respect to the future increase in CO_2 concentrations, we adopt the projections of Baes *et al.* (14). Those authors considered two scenarios, one in which fossil fuel consumption corresponding to the present-day growth rate of 4 percent is continued indefinitely, the second in which there is a 2 percent growth rate up to the year 2025 and a symmetrical decrease in growth rate thereafter. We will refer to the first as the fast growth and the second as the slow growth scenario. In addition, Baes *et al.* considered uncertainties about the percentage of the additional CO_2 that remains airborne. To estimate the range of CO_2 signal due to the resulting uncertainty in future airborne levels, we will consider as an upper limit the fast growth case with 60 percent airborne and as a lower limit the slow growth case with 40 percent airborne. Resulting CO_2 concentrations and values of g are shown in Table 1. It is assumed that CO_2 concentrations are known to 1975.

Comparing Signal and Noise

Although the positive-feedback models indicate that there is a seasonal variation in the strength of the predicted signal, the nature of this variation is not certain. Therefore we examine two possibilities: (i) the predicted maximum in signal occurs during summer and (ii) this maximum occurs during winter. First we consider the summer maximum case, for which the largest signal-to-noise ratios would be likely (15).

Before proceeding to compare signals with noise, it is important to consider the likely effect of bias in our estimates of this noise. Our time series consists of 72 years of data. We cannot adequately estimate variability on longer time scales, yet from Eq. 1 and Fig. 3 it is evident that the low-frequency variability becomes a major contributor to the variance for very long time averages. With admitted uncertainty, Kutzbach and Bryson (16) have attempted to mesh both instrumental and noninstrumental records in order to describe the low-fre-

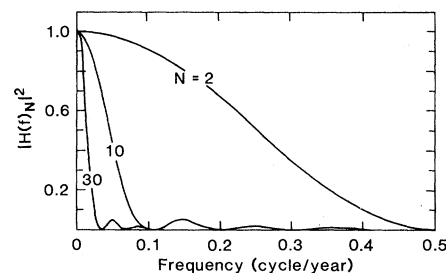


Fig. 3. Square of the amplitude response $|H(f)|^2$ for averages over $N=2, 10,$ and 30 years.

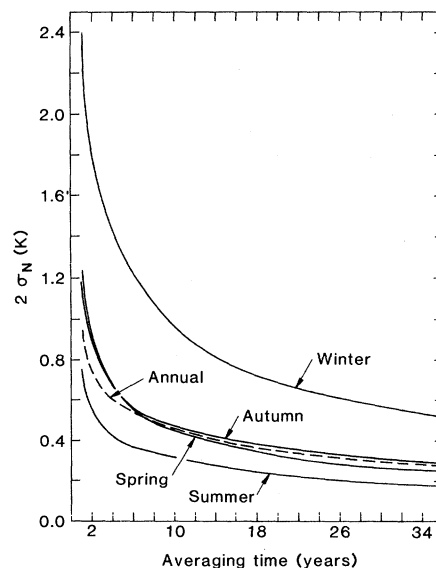


Fig. 4. Twice the expected standard deviations ($2\sigma_N$) for various averaging times N for each season and for annual averages. This is the estimated noise.

quency variance of winter temperature spectra. They found that the average spectral value between 100- and 1000-year periods is about twice that observed for periods near but shorter than 100 years. This gives us a basis for assessing the effect of bias on the summer curve of Fig. 4. If we were to model the summer spectrum between 0.01 and 0.001 cycle per year by twice the value shown in Fig. 2 in that frequency range, the level of $2\sigma_N$ shown in Fig. 4 would increase for 30-year averages ($N = 30$) by about 26 percent, from 0.19° to 0.24°C. The percentage increase would be less for shorter time averages and greater for longer time averages. The corresponding value of $2\sigma_{30}$ computed for the upper 95 percent limit of the summer spectrum shown in Fig. 2 is 0.34°C, nearly 80 percent larger than the 0.19°C computed from the spectrum itself. We tentatively conclude that, although our estimates of $2\sigma_N$ are probably biased downward, the effect is considerably smaller than that of the uncertainty due to sampling variability. This should be true for N on the order of 30 years, but bias probably becomes a more serious problem for N much larger than 30.

Figure 5, where Eq. 8 is combined with the summer curve from Fig. 4 (the summer noise), provides an estimate of when the predicted signal due to increasing CO_2 (obtained from Table 1) would exceed twice the estimated noise. The summer noise curve is taken directly from Fig. 4; the averaging time in years is indicated at the bottom, along with a date which is based on the assumption that averages begin in 1956 (17). The sig-

Table 1. CO_2 increase estimated from projections in (14). For 1985 and 1995 the upper limit (first value) is obtained from the fast growth (60 percent airborne) assumption and the lower limit (second value) is obtained from the slow growth (40 percent airborne) assumption.

Year	$[\text{CO}_2]$ (ppm)	$g =$ $[\text{CO}_2]/300$
Before 1930	300	1.0
1955	315	1.05
1965	321	1.07
1975	333	1.11
1985	360, 339	1.20, 1.13
1995	393, 348	1.31, 1.16

nal for the positive-feedback models is taken from the maximum value of $\Delta T_s(\theta)$ indicated in Eq. 8 for $\theta = 60^\circ\text{N}$. The signal for the zero-feedback models is taken from the corresponding minimum value indicated in Eq. 8. The signals are plotted against the time scale at the top of Fig. 5, neglecting any delays that might arise from the inertia of the climate system. Displacement of the signal scale (top) with respect to the noise scale (bottom) is necessary since, for example, a 20-year average from 1956 to 1975 would be an estimate of the 1965 signal. The two signal curves fan out after 1975 as a result of the uncertainty in future levels of airborne CO_2 . The upper limit reflects the fast growth, 60 percent airborne estimates and the lower limit the slow growth, 40 percent airborne estimates. The 95 percent limits about the noise curve (dotted lines) were determined from Eq. 1, with $S(f)$ taken from the 95 percent limits on the summer spectrum that are indicated in Fig. 2.

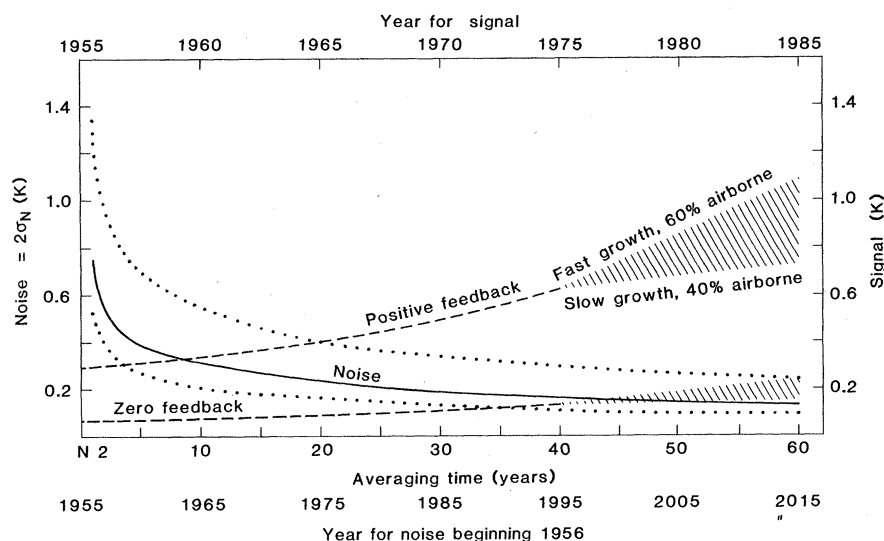


Fig. 5. Summer season $2\sigma_N$ from Fig. 4 (solid line) and 95 percent limits (dotted lines) plotted against averaging time and year beginning in 1956. Positive-feedback signal (upper dashed line) and zero-feedback signal (lower dashed line) are plotted against the year indicated at the top (see text for explanation of upper and lower year scales). Possible delays due to inertia of the climate system are not accounted for in the signal. Fanning out of the signal curves indicates the uncertainty of future CO_2 levels in the atmosphere; the upper values are based on fast growth with 60 percent CO_2 airborne and the lower values on slow growth with 40 percent airborne.

To interpret Fig. 5, we first assume that we know what the no-signal zonal mean temperature (the zonal mean temperature before any effect due to increasing CO_2) was, and that the noise curve does accurately depict the variability of time-averaged temperature that is not due to increasing CO_2 . Under these circumstances, we would conclude that a 9-year average of summer temperatures computed from 1956 through 1964 should come from a distribution with a mean that is displaced 2 standard deviations toward higher temperatures from the no-signal zonal mean if the positive-feedback models predict the effects of increasing CO_2 correctly. If the zero-feedback models are correct, it would require a 45-year average from 1956 through 2000 for a similar situation to occur. We interpret Fig. 5 as giving an approximate range of time when we might expect to be able to establish statistically that model predictions are correct. That range extends from the present if the positive-feedback models are correct to near the year 2000 if the zero-feedback models are correct. As it turns out, a 20-year average temperature from 1956 through 1975 is not higher than a 20-year average temperature from 1906 through 1925; in fact, it is slightly lower (14.2°C compared to 14.42°C). Therefore, we cannot provide statistical evidence that there has been an effect due to increasing CO_2 on the present mean zonal temperature at 60°N .

These results are summarized in Fig. 6 in the form of signal-to-noise ratios (signal/ $2\sigma_N$). Curves 1 and 5 come directly from Fig. 5 and depict the ratios for summer noise and the positive-feedback and zero-feedback signals, respectively. Because the seasonal dependence of positive-feedback signals is not adequately understood, we include three other curves in Fig. 6. Curve 4 is the positive-feedback signal from Fig. 5 divided by $2\sigma_N$ for winter seasons. This provides an estimate of the signal-to-noise ratio for winter if it turns out that the seasonal dependence is such that the maximum signal occurs in that season. If that proved to be the case, the corresponding signal for the other three seasons should be approximately given by (18)

$$\Delta T_s \approx 3 \ln g \quad (9)$$

Curve 2 is the signal-to-noise ratio for the resulting signal given by Eq. 9 and the summer noise. It is meant to approximate the signal-to-noise ratio for summer, for the case in which the seasonal dependence results in a maximum signal occurring not in summer, as in curve 1, but in winter. A comparison of curves 2 and 4 illustrates that, even in this case,

the signal-to-noise ratios would be larger in summer. Finally, curve 3 is based on an annual average signal given by

$$\Delta T_s = \frac{9 \ln g + 20 \ln g (1 - 1.4 \cos \theta)}{4} \quad (10)$$

Equation 10 is based on the assumption that the signal for three seasons is given by Eq. 9 and that for the fourth is given by Eq. 8. The noise is that determined for the annual averages. Since for $N > 6$ curves 1 and 2 fall above curves 3 and 4, we conclude that a CO₂ signal will be easiest to detect in summer unless its seasonal variation is significantly different from those considered here.

Like Fig. 5, Fig. 6 is based on the assumption that the thermal inertia of the climate system is zero. Thermal inertia would displace the curves to the right through a distance that depends on how much the signal in the surface temperature is delayed. For example, for a delay of 10 years, the signal-to-noise ratio for the signal from Eq. 9 and the summer noise would equal one around 1988 instead of 1977 as indicated by curve 2 in Fig. 6.

Discussion

The analysis of observed temperature variability at 60°N indicates that the surface warming predicted by current general circulation models of climate (19) should be evident now or at least within the next decade, depending on the seasonal dependence of the warming and on the ocean thermal inertia of the climate system. If the ocean thermal inertia does not delay the signal by more than a decade and the warming peaks in spring or summer, the surface warming should be detectable now. Since a recent 20-year average is not higher than a 20-year average from 1906 through 1925, we conclude that either such models overpredict the signal, or other compensatory climate changes are occurring. If the latter is not a serious problem and the warming is occurring at a rate lower than that predicted by GCM's but higher than that predicted by zero-feedback models, then it should be detectable anytime from the present to about the year 2000. In addition, we conclude that it will be easiest to detect effects in summer data.

We have assumed that all of the observed variance in the 72-year record is due to noise. The signal, if present in the data, would also contribute to the variance. Considering the positive-feedback signal to be very nearly a linear function of time, then it would contribute about 0.04 K² to the total variances of the time

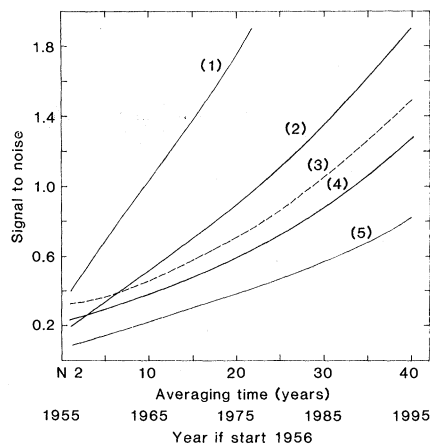


Fig. 6. Predicted signal divided by $2\sigma_N$ for (curve 1) feedback signal from Fig. 5 and $2\sigma_N$ for summer season from Fig. 4, (curve 2) signal from Eq. 9 and $2\sigma_N$ for summer season, (curve 3) average annual signal (see text) and $2\sigma_N$ for annual averages from Fig. 4, (curve 4) feedback signal from Fig. 5 and $2\sigma_N$ for winter season from Fig. 4, and (curve 5) zero-feedback signal from Fig. 5 and $2\sigma_N$ for summer season from Fig. 4. In computing signals we have neglected possible delays due to inertia of the climate system.

series (20) or 29 percent of the estimated summer noise of 0.14 K². This percentage would be larger for time-averaged data since the predicted slow temperature increase is essentially a low-frequency signal. However, attempting to isolate the noise by subtracting the predicted signal from the data beforehand increases the variance of the time series since there is no upward trend present. This brings us back to an important facet of the problem that cannot be neglected. Because our present knowledge of the causes of climate change is limited, it is difficult to distinguish between change that may be due to increasing CO₂ and change that is not. While it is reasonable to attempt to account for changes not due to CO₂ by looking at past records as we have done, we cannot be certain that such changes have not masked a CO₂ effect, or conversely that they may not indicate in the future that there is an observable effect of CO₂ when there is none. Because of this, as well as uncertainties in model predictions, unambiguous statistical proofs regarding the effects of CO₂ based on observations of a single variable will always be difficult. It may be necessary to look for physical as well as statistical evidence in order to adequately isolate and monitor possible effects of increasing CO₂. Physical evidence might be found in certain consistent relationships between two or more variables.

For example, as indicated by model studies, the increase in tropospheric temperature caused by CO₂ increase should be accompanied by a relatively

large cooling within the middle and upper stratosphere. Hence, we can look for out-of-phase changes between troposphere and stratosphere. However, the decrease in O₃ that is predicted due to continued use of chlorofluoromethanes (CFM's) can cause a stratospheric cooling of the same order of magnitude as the estimated CO₂ cooling (21), and this possibility must not be neglected.

Another approach would involve monitoring the radiation budget data obtained by satellites. Satellites measure the outgoing infrared flux (both integrated and spectral) and the solar flux reflected by the earth-atmosphere system. The predicted Δq should be seen as a reduction in the outgoing infrared flux between 13 and 17 micrometers, while the predicted increase in T_s caused by Δq would increase the outgoing flux in the rest of the infrared spectrum. If, on the other hand, the effect of CO₂ increase is compensated by other effects such as an increase in aerosols or low clouds, then the decrease in infrared flux between 13 and 17 will be compensated by an equivalent increase in the reflected solar flux. Conversely, if other anthropogenic effects (2) contribute appreciably to a future warming, such as increases in N₂O, CH₄, CFM's, and tropospheric O₃ (all of which have bands in the 8- to 12- μ m "window" region), there will be a corresponding decrease in the outgoing infrared flux in the window region.

Satellite measurements of adequate spectral resolution are available but, because of their limited accuracy and time history, they can only be used to detect effects of large CO₂ changes such as those expected to occur during the next century. We need to develop adequate strategies for summarizing and saving these valuable data for future use.

References and Notes

1. J. M. Mitchell, in *Workshop on the Global Effects of Carbon Dioxide from Fossil Fuels*, W. P. Elliott and L. Machta, Eds. (CONF-770385, UC-11, Department of Energy, Washington, D.C., 1979).
2. Some other potential causes of climate change are the following. (i) Anthropogenic sources: increases in CFM's enhance the atmospheric greenhouse effect in the spectral region 8 to 12 μ m. In addition, the CFM's may cause a reduction in O₃, which in turn can affect the climate. An increase in tropospheric O₃ due to CO and hydrocarbons, an increase in N₂O due to fertilizer use, and modification of the surface albedo by overgrazing and deforestation are among the important man-made forces that may affect climate. (ii) External boundary conditions: change in the solar constant and changes in stratospheric aerosol loading due to volcanic activity. By definition, one might consider any process whose time scale is long relative to daily weather fluctuations, such as sea-surface temperature and ice cover, to be external. (iii) Intransitivity [E. N. Lorenz, *Meteorol. Monogr.* 8, 1 (1968)]: this arises because the governing physical laws may allow more than one set of long-term statistics.
3. Observed variance is sometimes assumed to reflect potentially predictable shifts in climate means as well as unpredictable fluctuations in finite-time average estimates of those means. The

latter component is referred to as noise [C. E. Leith, *J. Appl. Meteorol.* **12**, 1066 (1973); R. A. Madden, *Mon. Weather Rev.* **104**, 942 (1976); and D. J. Shea, *ibid.* **106**, 1695 (1978)].

This distinction need not be made here, since the possible effects of increasing CO₂ must be isolated from the total interannual variability regardless of its ultimate origin.

4. R. H. Jones, *J. Appl. Meteorol.* **14**, 159 (1975).
5. G. M. Jenkins and D. G. Watts, *Spectral Analysis and Its Applications* (Holden-Day, San Francisco, 1968), pp. 244-252.
6. J. M. Mitchell, *Quat. Res. (N.Y.)* **6**, 481 (1976).
7. R. B. Blackman and J. W. Tukey, *The Measurement of Power Spectra from the Viewpoint of Communications Engineering* (Dover, New York, 1958), pp. 25 and 112.
8. V. Ramanathan, M. S. Lian, R. D. Cess, *J. Geophys. Res.* **84**, 4949 (1979).
9. T. Augustsson and V. Ramanathan [*J. Atmos. Sci.* **34**, 449 (1977)] show that the various radiative-convective model studies yield values for enhanced CO₂ radiative heating that agree with each other within 10 percent. On this basis, we conservatively assume an uncertainty of approximately ± 20 percent due to radiation model errors.
10. The upper limit for λ_0 ($\approx 4 \text{ W m}^{-2} \text{ K}^{-1}$) is obtained by assuming that the climate system is devoid of all feedbacks other than infrared radiative damping and that it emits infrared radiation like a blackbody with an equilibrium temperature of about 255 K. One-dimensional radiative-convective models yield values of λ_0 ranging from 1.25 to $2 \text{ W m}^{-2} \text{ K}^{-1}$ [V. Ramanathan and J. A. Coakley, *Rev. Geophys. Space Phys.* **16**, 465 (1978)]. Energy balance climate models yield λ_0 values ranging from 1 to $2 \text{ W m}^{-2} \text{ K}^{-1}$ [for example, see M. S. Lian and R. D. Cess, *J. Atmos. Sci.* **34**, 1058 (1977)], from which we obtain the lower limit of λ_0 shown in Eq. 4. The principal

reason why the model λ_0 values are significantly smaller than $4 \text{ W m}^{-2} \text{ K}^{-1}$ is the inclusion of relative humidity feedback [see the Ramanathan and Coakley reference cited above] and the ice-albedo feedback [see the Lian and Cess reference cited above]. The effects of these two positive feedbacks may be compensated by as yet unidentified negative feedbacks involving cloud-radiative interactions and ocean-atmosphere interactions.

11. S. Manabe and R. T. Wetherald, *J. Atmos. Sci.* **32**, 3 (1975).
12. V. Ramanathan, *ibid.* **34**, 1885 (1977).
13. S. L. Thompson and S. H. Schneider, *J. Geophys. Res.* **84**, 2401 (1979); B. G. Hunt and N. C. Wells, *ibid.*, p. 787.
14. C. F. Baes, H. E. Goeller, J. S. Olson, R. M. Rotty, *Oak Ridge Natl. Lab. Rep. ORNL-5194*, (1976).
15. From Fig. 2, we saw that annual averages have larger noise than summer averages. We also computed 9-month averages from March through November, excluding the winter months. The resulting variance is slightly less than that for the 3-month summer averages (0.13 compared to 0.14 K²); however, the spectrum of the 9-month averaged data has relatively more variance at low frequencies than that of the summer-averaged data, so that averaging several summers together decreases the noise variance faster than averaging several 9-month means together. As a result, we believe that the 3-month summer seasons provide the data set with the least noise.
16. J. E. Kutzbach and R. A. Bryson, *J. Atmos. Sci.* **31**, 1958 (1974).
17. Results did not appear to be particularly sensitive to assumed starting date. For example, when averages are computed from 1930, the positive-feedback signal crosses the $2\sigma_N$ noise line in 1960 (30-year average) and the zero-feed-

back signal is still below the line in 1990 (50-year average). By beginning averages in 1956, we can avoid some of the uncertainties which bias in the near-zero frequency spectral estimates introduced into longer time averages with virtually no change in the result.

18. In this case, since we have assumed that the ΔT_s amplification due to ice-albedo feedback is manifested during winter, the summer signal is that given by the positive-feedback models without the ice-albedo feedback. The λ_0 for the positive-feedback models without ice-albedo feedback is approximately $2 \text{ W m}^{-2} \text{ K}^{-1}$, and hence Eq. 9 is obtained by combining Eqs. 2 and 4 with $\lambda_0 = 2 \text{ W m}^{-2} \text{ K}^{-1}$. Also, the results for this case closely resemble those obtained by S. Manabe and R. J. Stouffer [*Nature (London)* **282**, 491 (1979)]. In their coupled GCM-simple mixed-layer ocean model, Manabe and Stouffer found, at 60°N for $g=4$, a winter warming of about 10 K and a summer warming of 4 K. Equations 7 and 9 give similar values of 8.3 and 4.2 K.
19. Several unpublished GCM studies of the CO₂ climate problem are summarized in a recent report [Ad Hoc Study Group on Carbon Dioxide and Climate, *Carbon Dioxide and Climate: A Scientific Assessment* (Climate Research Board, National Research Council, Washington, D.C., 1979)]. As seen from this report, the high-latitude surface warming predicted by the GCM's is of the same magnitude or larger than the upper limit for ΔT_s given in Eq. 8.
20. From Fig. 5 the positive-feedback signal is about 0.70 K in 1977. Since the signal is nearly a linear function of time, it would contribute $(0.7 \text{ K})^{2/12}$ to the variance.
21. V. Ramanathan and R. E. Dickinson, *J. Atmos. Sci.* **36**, 1084 (1979).
22. We thank S. Schneider and H. van Loon for their helpful comments on an earlier version of this article.

Teratocarcinomas and Mammalian Embryogenesis

Gail R. Martin

Teratomas have always intrigued pathologists because they contain a grotesque array of diverse tissues, sometimes including highly organized structures such as teeth, fingers, and hair. Thanks to the pioneering work of Stevens (1), these rare tumors have become more than a curiosity of human pathology. Stevens observed that mice of certain inbred strains frequently develop tumors analogous to human teratomas. His subsequent studies provided a clear understanding of how teratomas arise in mice and perhaps in man as well. As cell lines were established from the mouse tumors that Stevens made available, it became apparent that these cultured cells (known as embryonal carcinoma

cells or teratocarcinoma stem cells) are remarkably similar to the cells of the early embryo. The use of these tumor cells as a model system for the study of mammalian development in vitro circumvents many of the difficulties of working with embryonic material. Interest was further stimulated by the demonstration that embryonal carcinoma cells taken from the tissue culture dish can participate in the formation of a normal mouse. Such results have raised the hope that teratocarcinoma cells will be useful in creating mouse models of human genetic diseases. The discussion in this article centers on what teratocarcinoma stem cells are and on some of the ways in which their potential uses have been exploited.

Pluripotency and origin of teratocarcinoma stem cells. A typical mouse tera-

toma or teratocarcinoma contains a mixture of differentiated cell types (Fig. 1A). This complexity is accounted for by the fact that these tumors arise from stem cells that are pluripotent (2); that is, they are capable of forming derivatives of all three primary germ layers, namely, endoderm, mesoderm, and ectoderm. The random array of differentiated tissues forms as some stem cells differentiate into cartilage, and others into nerve, muscle, glandular tissue, or other cell types. It is not yet known what triggers such differentiation, but in general the differentiated derivatives of the stem cells are normal, nonmalignant cells (3).

Some stem cells, instead of differentiating, continue to proliferate in the undifferentiated state. They thus form nests of pluripotent embryonal carcinoma cells interspersed in the disorganized mixture of differentiated derivatives (Fig. 1B). The continued proliferation of this undifferentiated stem-cell population is responsible for the malignant properties of teratocarcinomas such as progressive growth and transplantability, but not metastasis (4). In cases where the stem cells cease to proliferate because they differentiate or die, the tumors become benign and are known as teratomas. Strictly speaking, "teratocarcinoma" refers to a malignant tumor, and "teratoma" refers to a benign one. The latter term, however, is often used to designate either type of tumor.

The author is an assistant professor in the Department of Anatomy, School of Medicine, University of California, San Francisco 94143.